

Colloidal matter separation of industrial wastewaters from Galați City area by semipermeable membranes

Aurel TĂBĂCARU, Simona BUTAN, and Romică CREȚU*

Department of Chemistry, Physics and Environment, Faculty of Sciences and Environment, "Dunărea de Jos" University of Galați, 111 Domneasca Street, 800201, Romania

Abstract. Various studies have shown that ultrafiltration membranes are successfully involved in the removal process of most organic pollutants from wastewater. In this context, the hydrodynamic characteristics of a modified cellulose ultrafiltration membrane were evaluated. This composite membrane type has been proposed for the separation of colloidal matter from industrial wastewater in Galați City area (Romania). Another purpose of this paper was also to determine the volume flows, along with the permeate and concentrate fluxes through the technical membrane taken under study. Furthermore, a comparative analysis of three samples of industrial water from Galați City area in terms of the degree of contamination was performed. Surface modification was evaluated using scanning electron microscopy. Results indicated that the industrial wastewater from the steel factory Liberty Galați was significantly more impure than the water from Cătușa Lake, which in turn was more impure than the water from Siret River, as indicated by comparative analysis of the water samples subjected to the ultrafiltration operation through semipermeable technical membranes. It was shown that the decrease of the permeate flux at the modified cellulosic membrane was accentuated in the first moments, probably due to the clogging of the surface pores that present an uneven distribution. The results of the present study show that the cellulosic membrane used has pore diameters which correspond to the values recommended for the retention of colloidal matter.

Keywords: ultrafiltration; UF membrane; scanning electron microscopy; permeate and concentrate fluxes.

1. Introduction

Lately, wastewater from various industrial and domestic activities has become a major environmental problem. Therefore, various wastewater-cleaning technologies using ultrafiltration (UF) membranes have been developed [1]. UF membranes are involved in removing process of most organic pollutants, microbiological species and certain metals (Mn, Hg, Cr, Cd, Pd, Ni, Zn) from wastewater, with low energy consumption and a simple operating system [2-4]. The use of these UF membranes to clean wastewater is disturbed by the fouling process. The fouling prevention can be achieved using microalgae or zwitterion-containing polymer additives [5, 6]. The fouling process is closely correlated to membrane cleaning, which involves several physical, chemical and biological cleaning steps depending on the UF membrane molecular weight cut-offs [7-9].

Recently, certain methods to obtain selective and fouling resistant UF membranes have been improved according to polymeric membranes used. The most commonly used polymer to develop these membranes is polyvinyl chloride (PVC), which has essential chemical and mechanical properties, such as chemical and thermal stability, abrasion and corrosion resistance and a suitable mechanical strength [10]. To increase the antifouling and mechanical properties of UF membranes, particular procedures are used, such as, different changes of membrane surface, incorporation of

specific nanoparticles into membrane matrix and polymers blending [11-13].

A challenging polymer that can be used in UF membranes design is cellulose acetate, which is a low-cost and renewable resource, with significant biodegradable properties. The antifouling and separation characteristics of cellulose acetate UF membranes can be enhanced using zinc oxide ZnO@graphitic carbon nitride (g-C₃N₄) nanocomposites [14] or silver nanoparticles [15]. However, cellulose UF membranes have some disadvantages, such as high sensitivity to bacterial corrosion and lack of mechanical tolerance leading to loss of life [16].

A key feature of UF membrane development based on the mixture of several polymers (polysulfone/polyaniline, PVC or cellulose acetate) is the influence of pH, temperature and KMnO₄ peroxidation effect [17]. The suitable UF membranes used for wastewater treatment are obtained at an optimal value of pH equal to 7 and a moderate temperature (25°C) [18].

In the present work, we introduce a cellulosic membrane into the separation practice by UF process of three distinct water samples from Galați city area, namely: water from Siret River, water from Cătușa Lake and industrial water from the steel factory Liberty Galați. Besides the evaluation of the hydrodynamic characteristics of the membrane type used, the aim of this paper is also to determine the volume flows, along

*Corresponding author. *E-mail address:* romica.cretu@ugal.ro (Romică Crețu)

with the permeate and concentrate fluxes through the semipermeable technical membrane taken under study, and then to perform a comparative analysis of the three water samples in terms of the degree of pollution and contamination for each sample. The experimental conditions in this paper correspond to the UF process, and therefore, in the following we will refer only to this type of technical separation.

2. Experimental

2.1. Determination of the membrane's characteristics

For the determination of volume flow (Q_v), permeate volume flux (J_p) and concentrate volume flux (J_c) of the four different water samples, a technical semipermeable cellulose membrane composite, type M110 (produced by Ceprohart Brăila) was used. It has the effective diameter of separation $d_e = 10$ cm and the thickness $h = 3.6$ mm.

The total porous volume (V_{pt}) of the semipermeable membrane was calculated with Equation 1:

$$V_{pt} = \frac{m_w - m_d}{\rho_w} \quad (1)$$

which, in turn, served to calculate the apparent porosity of the membrane with Equation 2:

$$\varepsilon, \% = \left(1 - \frac{V_{pt}}{V_m}\right) \times 100 \quad (2)$$

where: m_w is the mass of the membrane soaked in distilled water of density $\rho_w = 1$ g/cm³; m_d is the mass of the dried membrane (weighed in the air); $V_m = \frac{m_d}{\rho_m}$ is the volume of the membrane of density ρ_m .

For the determination of the *total porous volume*, the AG4-Mettler Toledo balance was used. To this aim, the mass of the dried membrane was $m_d = 16.61$ g and the mass of the membrane soaked in distilled water was $m_w = 43.57$ g. Thus, the total porous volume of the membrane was $V_{pt} = 26.96$ cm³.

For the calculation of the *apparent porosity* of the membrane, it was necessary to calculate first the volume of the membrane (V_m), knowing its diameter and thickness, that is $V_m = \frac{\pi \times d^2}{4} \times h = 28.274$ cm³. Thus,

the apparent porosity of the membrane was $\varepsilon, \% = 33.749\%$.

For the calculation of volume flow (Q_v) and volume fluxes (J_p and J_c), it also was necessary to calculate the effective separation area of the membrane, $A = \frac{\pi \times d_e^2}{4}$, that is $A = 78.5$ cm².

For the analysis of surface morphology of the membrane, scanning electron microscopy (SEM) images were collected on a Quanta 200 scanning electron microscope operating at different voltages in the range 10–30 kV.

2.2. Laboratory setup for the ultrafiltration of water samples

The laboratory setup used for the UF operation of the water samples by semipermeable membranes is presented in Figure 1. This setup allows: *i*) the determination of porosity and maximum radii of UF membranes, *ii*) establishing the retention coefficients or cut-off molecular weights, *iii*) characterization of the separation performances by a certain technical membrane, and *iv*) evaluation of the separation efficiency by UF of diverse colloidal dispersions.

The supply fluid from tank (1) is taken by the dosing pump (3), whose flow is adjusted with the micrometric screw (4), and enters the measuring block for pressure and temperature (5), from which it goes tangentially on the membrane surface from module (6). Here, the separation of the two fluxes – concentrate (10) and permeate (12) – takes place. The working maximum pressure is 10 atm and the maximum flow of the supply fluid is 25 L/h at a temperature of up to 75°C. Figure 2 gives the constructive principle of an UF module, which can also be used in microfiltration. It is a closed, watertight enclosure in which the membrane (4) is placed with the support for mechanical strength (3) and for the drainage of the permeate (nickel sieve). The module has a turbulent flow pressure supply system and connections for concentrate and permeate collection. Two or more modules can be connected in series, in parallel or in combination, depending on the separation conditions and the retentate (often permeate) recirculation system.

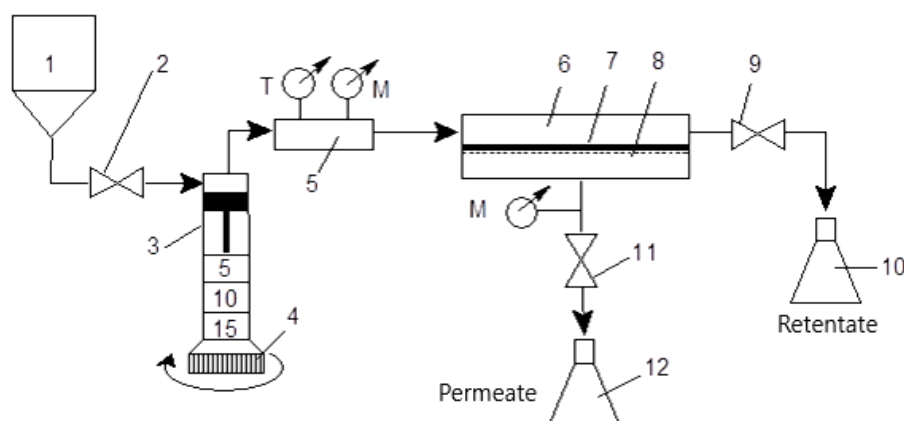


Figure 1. Laboratory setup for separations by technical membranes: 1 – Supply tank; 2, 9, 11 – Control valves; 3 – Dosing pump; 4 – Micrometric screw for flow adjustment; 5 – Measuring block; 6 – Filtering module; 7 – Membrane; 8 – Metallic stand; 10, 12 – Collecting vessels for retentate (concentrate) and permeate.

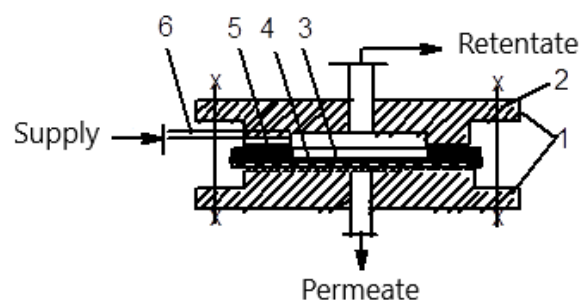


Figure 2. Scheme of the UF module: 1 – Detachable ribbed tiles; 2 – Clamping screws; 3 – Nickel sieve; 4 – Membrane; 5 – Rubber seal; 6 – Fitting.

2.2. Working procedure

1. Establishing the characteristics of the dosing pump (3): the filtering module (6) is removed and the volumes of distilled water and the other water samples taken under study, discharged by the pump for position 5 of the micrometric screw (4), are measured with a graduated cylinder. The permeate volume flow (Q_p) and the concentrate volume flow (Q_c) are calculated with Equations 3, while the permeate volume flux (J_p) and the concentrate volume flux (J_c) are calculated with Equations 4:

$$q_p = \frac{V_p}{\Delta t} \text{ and } Q_c = \frac{V_c}{\Delta t} \quad (3)$$

$$J_p = \frac{Q_p}{A} \text{ and } J_c = \frac{Q_c}{A} \quad (4)$$

2. Mounting the membrane into the UF module is detailed in Figure 2. The membrane (4) is placed on the nickel sieve (3). The rubber seal (5) is fixed onto the membrane the superior tile (1) is attached and tighten crosswise with the screws (2) to ensure pressure sealing. The module is connected to the measuring block (5) in

Figure 1 with the fitting (6) with Dutch nut. Above the membrane is a clear height of 2.4 mm. The flow is turbulent due to the streaks on the top plate.

The variation of the permeate and concentrate fluxes (calculated with Equations 4) of distilled water and test samples as a function of time is plotted. Once the fluxes are flattened, it is considered that the concentration polarization has been installed and the membrane must be regenerated with distilled water.

Statistical analysis was performed using the SPSS 11.0 software. All statistical analyses were statistically significant at the confidence level of 0.05 [19, 20].

3. Results and discussion

3.1. Membrane characterization

The information obtained by scanning electron microscopy showed the difference from a morphological point of view in the case of the cellulosic porous membrane M110 as a result of the passage of the fluid (distilled water) used as a standard (Figure 3).

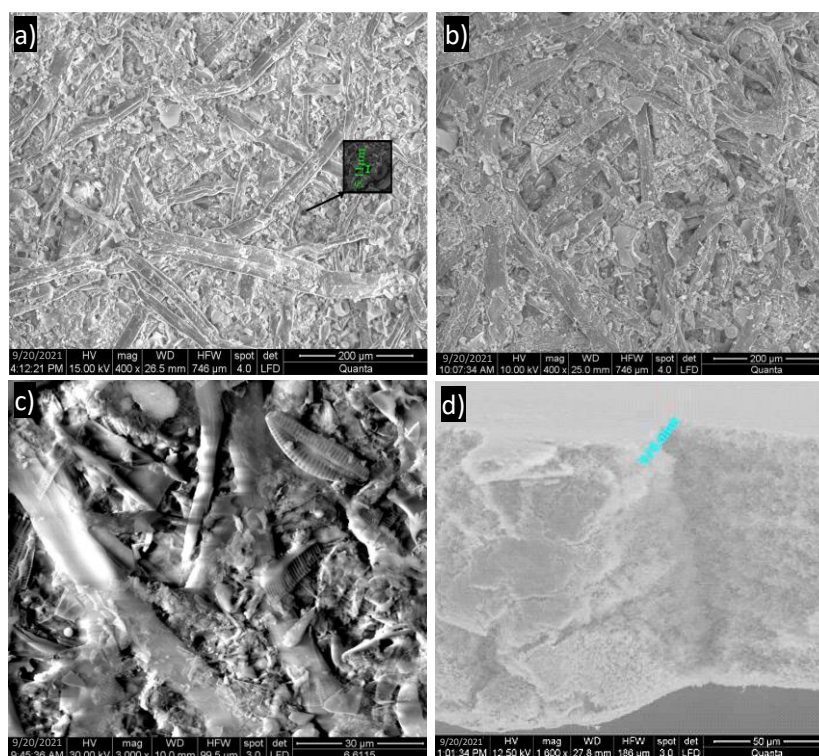


Figure 3. SEM images of the inlet (a) and outlet (b) surfaces of distilled water into the composite cellulosic membrane M110 (400x magnification) used to separate the water samples from Siret River, Cătușa Lake, and industrial wastewater from the steel factory Liberty Galați; (c) SEM image of the distilled water outlet surface through the membrane M110 (3000x magnification); (d) SEM image of the cross section of the layer details of the membrane M110 (1600x magnification).

The images in Figure 3 show the initial relative dimensional uniformity of the cellulosic fibers in the M110 membrane, highlighting the role of the cellulosic fibrous network in filtering the various substances that constitute the impurities contained in the analyzed samples and that significantly change its porosity. In this context, the morphology of the upper surface of the filter plate used in this study showed, after filtration, different characteristics compared to the original membrane (results are not shown). The data obtained show that the fibers with non-uniform orientation have different thicknesses and lengths, so that the membrane surface has a variable pore distribution, with diameters of the inlets in the surface pores of the membrane ranging from a few μm to about $300 \mu\text{m}$, reaching up to over 900 nm . The active surface of the membrane has an apparent porosity of 33.749% , which brings the membrane in the range from micro to ultrafiltration.

3.2. Experimental determinations of the ultrafiltration process

The data provided by SEM are verified by the hydrodynamic characteristics of the filter membrane. Thus, in Tables 1 – 4 are shown the experimental determinations performed for the four water samples subjected to the UF process using the laboratory setup

described in section 2.2, working at a pressure of 1 atm and a flow rate of the dosing pump of 5 mL/s .

Table 1. Experimental results for distilled water

Det. No.	V_p (mL)	τ (min)	Q_p (L/s)
1.	22	1	$0.366 \cdot 10^{-3}$
2.	22	2	$0.366 \cdot 10^{-3}$
3.	21.5	3	$0.358 \cdot 10^{-3}$
4.	21	4	$0.350 \cdot 10^{-3}$
5.	21	5	$0.350 \cdot 10^{-3}$
6.	21	6	$0.350 \cdot 10^{-3}$

Table 2. Experimental results for the water sample from Siret River

Det. No.	V_p (mL)	V_c (mL)	τ (min)	Q_p (L/s)	Q_c (L/s)
1.	12	18	1	$0.2 \cdot 10^{-3}$	$0.3 \cdot 10^{-3}$
2.	11.5	17.5	2	$0.19 \cdot 10^{-3}$	$0.29 \cdot 10^{-3}$
3.	11	17	3	$0.18 \cdot 10^{-3}$	$0.28 \cdot 10^{-3}$
4.	10.5	16.5	4	$0.17 \cdot 10^{-3}$	$0.27 \cdot 10^{-3}$
5.	10	16	5	$0.16 \cdot 10^{-3}$	$0.26 \cdot 10^{-3}$
6.	10	15.5	6	$0.16 \cdot 10^{-3}$	$0.25 \cdot 10^{-3}$

Table 3. Experimental results for the water sample from Cătușa Lake

Det. No.	V_p (mL)	V_c (mL)	τ (min)	Q_p (L/s)	Q_c (L/s)
1.	9	23	1	$0.15 \cdot 10^{-3}$	$0.38 \cdot 10^{-3}$
2.	8.5	22.5	2	$0.14 \cdot 10^{-3}$	$0.37 \cdot 10^{-3}$
3.	8	22.5	3	$0.13 \cdot 10^{-3}$	$0.37 \cdot 10^{-3}$
4.	7.5	22	4	$0.12 \cdot 10^{-3}$	$0.36 \cdot 10^{-3}$
5.	7	21	5	$0.11 \cdot 10^{-3}$	$0.35 \cdot 10^{-3}$
6.	7	19.5	6	$0.11 \cdot 10^{-3}$	$0.32 \cdot 10^{-3}$

Table 4. Experimental results for the industrial wastewater sample collected from the discharge line of the steel factory Liberty Galați

Det. No.	V_p (mL)	V_c (mL)	τ (min)	Q_p (L/s)	Q_c (L/s)
<i>Before coagulation</i>					
1.	9.2	16.5	1	$0.153 \cdot 10^{-3}$	$0.275 \cdot 10^{-3}$
2.	10.2	15.5	2	$0.17 \cdot 10^{-3}$	$0.258 \cdot 10^{-3}$
3.	10	16.5	3	$0.166 \cdot 10^{-3}$	$0.275 \cdot 10^{-3}$
4.	10.2	15.5	4	$0.17 \cdot 10^{-3}$	$0.258 \cdot 10^{-3}$
5.	10	15.5	5	$0.166 \cdot 10^{-3}$	$0.258 \cdot 10^{-3}$
6.	10	15.5	6	$0.166 \cdot 10^{-3}$	$0.258 \cdot 10^{-3}$
7.	10.6	16	7	$0.176 \cdot 10^{-3}$	$0.266 \cdot 10^{-3}$
8.	10.6	15.5	8	$0.176 \cdot 10^{-3}$	$0.258 \cdot 10^{-3}$
<i>After coagulation with FeCl_3 solution and NaOH 33% solution</i>					
1.	14.4	11	1	$0.240 \cdot 10^{-3}$	$0.183 \cdot 10^{-3}$
2.	14.4	11	2	$0.240 \cdot 10^{-3}$	$0.183 \cdot 10^{-3}$
3.	14.6	10	3	$0.243 \cdot 10^{-3}$	$0.166 \cdot 10^{-3}$
4.	14.8	9.5	4	$0.246 \cdot 10^{-3}$	$0.158 \cdot 10^{-3}$
5.	15.4	9	5	$0.256 \cdot 10^{-3}$	$0.150 \cdot 10^{-3}$
6.	15.6	8.5	6	$0.260 \cdot 10^{-3}$	$0.143 \cdot 10^{-3}$
7.	17.4	9.5	7	$0.290 \cdot 10^{-3}$	$0.158 \cdot 10^{-3}$
8.	16.4	9.5	8	$0.273 \cdot 10^{-3}$	$0.158 \cdot 10^{-3}$
9.	15.4	9	9	$0.256 \cdot 10^{-3}$	$0.150 \cdot 10^{-3}$
10.	14.8	8.5	10	$0.246 \cdot 10^{-3}$	$0.143 \cdot 10^{-3}$

The data presented in Tables 1 – 4 suggest the separating effect when using this type of membrane,

which has a high capacity to retain solids and contaminants in the UF process. Moreover, the

correlation coefficients between the values of the hydrodynamic parameters in the case of the filter membrane and the time corresponding to the

experiments for the studied water types (Table 5) showed that there are significant correlations between them for all analyzed water samples.

Table 5. Pearson linear correlation coefficients between the values of the hydrodynamic parameters ^{a,b,c,d} in the case of the membrane M110

	V _p	V _c	τ	Q _p	Q _c	J _p	J _c
^a water from Siret River							
V _p	1.000						
V _c	0.982	1.000					
τ	-0.982	-1.000	1.000				
Q _p	1.000	0.982	-0.982	1.000			
Q _c	0.982	1.000	-1.000	0.982	1.000		
J _p	1.000	0.983	-0.983	1.000	0.983	1.000	
J _c	0.980	0.999	-0.999	0.980	0.999	0.981	1.000
^b water from Cătușa Lake							
V _p	1.000						
V _c	0.852	1.000					
τ	-0.982	-0.929	1.000				
Q _p	0.999	0.852	-0.982	1.000			
Q _c	0.841	0.994	-0.925	0.841	1.000		
J _p	0.999	0.852	-0.982	0.999	0.841	1.000	
J _c	0.838	0.994	-0.924	0.838	0.999	0.839	1.000
^c industrial wastewater before coagulation							
V _p	1.000						
V _c	-0.531	1.000					
τ	0.767	-0.477	1.000				
Q _p	0.999	-0.542	0.747	1.000			
Q _c	-0.543	0.999	-0.489	-0.554	1.000		
J _p	0.998	-0.550	0.737	0.999	-0.562	1.000	
J _c	-0.542	1.000	-0.488	-0.554	0.999	-0.562	1.000
^d industrial wastewater after coagulation with FeCl ₃ solution and NaOH 33% solution							
V _p	1.000						
V _c	-0.514	1.000					
τ	0.747	-0.764	1.000				
Q _p	0.999	-0.504	0.739	1.000			
Q _c	-0.521	0.999	-0.772	-0.511	1.000		
J _p	0.999	-0.505	0.739	0.999	-0.511	1.000	
J _c	-0.521	0.999	-0.772	-0.511	0.999	-0.512	1.000

These results suggest that the study of the filtration process by using advanced methods of statistical analysis of hydrodynamic parameters characteristic of cellulosic porous membranes is efficient and allows the optimal evaluation of their quality

3.3. Interpretation of the experimental results

Figure 4 shows graphically the variation of the permeate flux as a function of time for distilled water considered a standard sample, which is chemically pure and with a zero degree of pollution. Therefore, the volume of permeate passing through the pores of the membrane used, respectively the permeate flux J_p , is the largest compared to the other water samples analyzed. The graph shown in Figure 4 shows a decrease in the permeate flux J_p to a value corresponding to minute 4

when it no longer decreases and therefore remains constant.

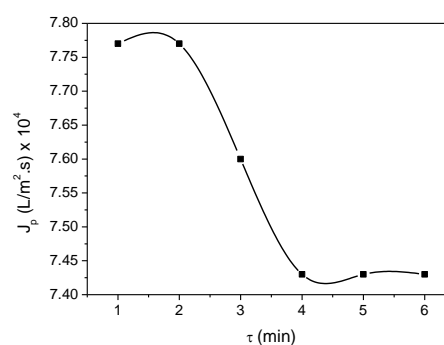


Figure 4. Variation of the permeate volume flux in time for distilled water

Figure 5 shows graphically the variation of the permeate flux and the concentrate flux as a function of time for the water sample taken from Siret River, from which an approximately linear decrease of the two fluxes, J_p and J_c , is observed. The volume of permeate passing through the membrane is this time smaller than in the case of the distilled water sample, which already indicates the existence of a certain degree of pollution and the presence of suspended impurities, which are retained to some extent by the membrane pores.

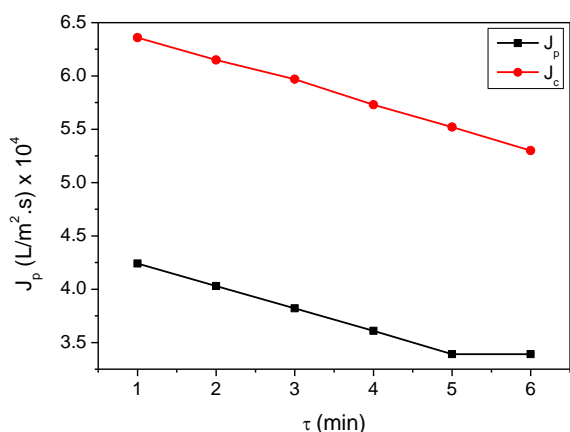


Figure 5. Variation of the permeate and concentrate fluxes in time for the water sample taken from Siret River

Figure 6 shows graphically the variation of the permeate and concentrate fluxes as a function of time for the water sample taken from Cătușa Lake, from which an approximately linear decrease of the two fluxes is observed. The volume of permeate passing through the membrane is smaller than in the case of the water sample from Siret River, which indicates that the water from Cătușa Lake is more impure than the water from Siret River.

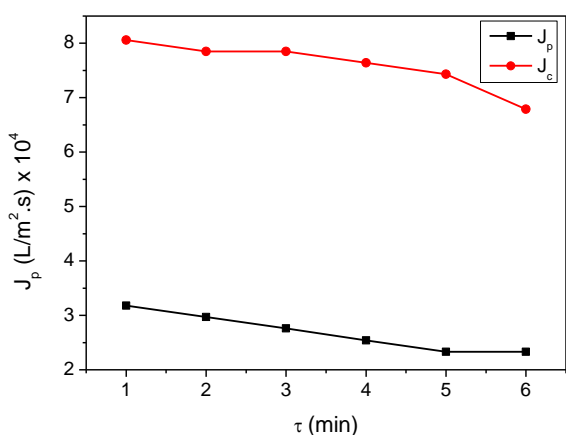


Figure 6. Variation of the permeate and concentrate fluxes in time for the water sample taken from Cătușa Lake

Figures 7 and 8 show the variation of the permeate and concentrate fluxes as a function of time for the industrial wastewater sample taken from the discharge line of the steel factory Liberty Galați, before coagulation and after coagulation, respectively. The graph shown in Figure 7 shows a discontinuous variation of the two fluxes, respectively of the permeate and concentrate volumes. This leads to the probable idea that some of the pores of the membrane used, during the UF process, clog and then unclog, which is why the

variation of the flux, respectively of the permeate volume, no longer occurs continuously. At the same time, the volume of permeate passing through the membrane is slightly higher, in average value, than in the case of the water sample from Cătușa Lake, which shows a higher amount of colloidal substances.

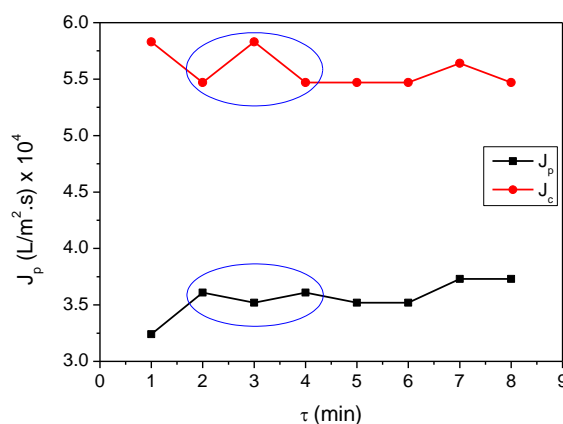


Figure 7. Variation of the permeate and concentrate fluxes in time for the industrial wastewater sample taken from Liberty Galați (before coagulation)

In a more detailed analysis, Figure 7 shows that after a 2 minutes contact between the industrial water and the membrane pores, the permeate flux decreases, while the concentrate flux increases, after which a period of stationarity is installed in the mass transfer through the membrane. The decrease in the filtrate flux is primarily due to the formation of the clogging layer specific to conventional filtration. It, in turn, is dependent on the retention of solid particles and the adsorption of pollutants in colloidal form on the fibrous cellulosic network, which significantly modifies its porosity and, therefore, the hydrodynamic characteristics. The retention of colloidal substances by the M110 filter membrane is neither selective nor limiting. This depends only on the separation capacity of the formed clogging layer. Also, after about 7 minutes from the beginning of the experiment, the two fluxes, permeate and concentrate, respectively, begin to differ more pronounced, probably due to the appearance of larger pressure differences.

After the coagulation of the respective water sample, it is observed, from the graph shown in Figure 8, an increase of the permeate flux to a certain maximum value after which it starts to decrease continuously, whereas the concentrate flux undergoes a decrease to a certain minimum value after which it starts to fluctuate slightly. Figure 8 is eloquent regarding the effect of coagulation on the flux through the porous membrane.

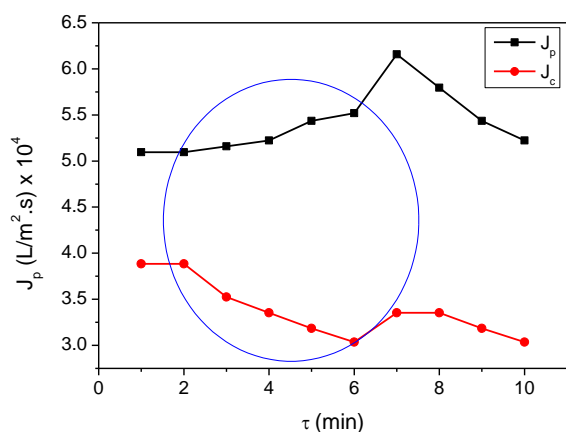


Figure 8. Variation of the permeate and concentrate fluxes in time for the industrial wastewater sample taken from Liberty Galați (after coagulation)

On the other hand, the volume of permeate through the membrane has now become higher after coagulation, indicating that there has been a decrease in the degree of pollution and the amount of impurities, compared to the water sample before coagulation. The increase of J_p to a certain maximum value followed by its continuous decrease leads to the idea that, after coagulation, the respective water sample being partially cleaned of the suspended substances, registered after the separation through the membrane an increase of the permeate volume. After the membrane pores began to become partially clogged with the remaining impurities, probably remaining in the sample after coagulation, this permeate volume began to decrease continuously. The flux decreases because it is proportional to the value of the driving force of the separation (pressure difference) and inversely proportional to the sum of all the resistance forces that oppose the mass transfer.

The comparative study of the variation in time of the permeate flux in the case of the five types of water samples subjected to the UF process by the cellulosic porous membrane M110 is presented in Figure 9.

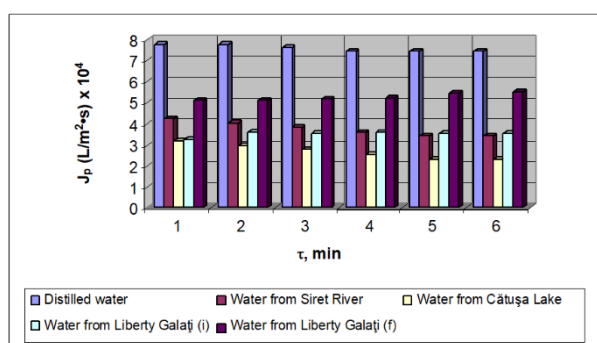


Figure 9. Dynamics of the permeate flux for the studied water samples

Overall, it can be observed that the permeate fluxes emerged from UF correspond to the porometric date, as well as the membrane morphology identified through SEM analysis.

4. Conclusions

The comparative analysis of the three water samples subjected to the UF operation through semipermeable technical membranes led to the conclusion that, from the

point of view of the presence of colloidal substances, the industrial wastewater from the steel factory Liberty Galați is significantly more impure than the water from Cătușa Lake, which in turn is more impure than the water from Siret River. This analysis was evident against the distilled water taken as a standard for which the volume of permeate through the membrane is the highest. The decrease of the permeate flux at the studied membrane is accentuated in the first moments due to the clogging of the surface pores that present an uneven distribution, aspect confirmed by the experiments related to the reference water.

Colloidal matter separation of industrial wastewaters, by the process of UF through technical membranes can be considered more advantageous and more rigorous compared to conventional filtration, because semipermeable membranes, through their very small pores, have the ability to retain as much impure substances in suspension. Membrane separation is optimal when it can more easily transfer one component to another. The UF operation will stop after the pronounced decrease of J_p and the membrane porosity will be restored.

The fact that the volume of permeate for the water sample from Liberty Galați after coagulation increased compared to the other water samples analyzed, finally leads to the idea that the UF operation through semipermeable technical membranes can be used as an alternative in the separation processes and purification of wastewater with a high degree of pollution and contamination. The results of the present study show that the cellulosic membrane used has pore diameters which correspond to the values recommended for the retention of colloidal matter.

Conflict of interest

Authors declare no conflict of interest.

References

- [1]. S. Al Aani, T.N. Mustafa, N. Hilal, Ultrafiltration membranes for wastewater and water process engineering: A comprehensive statistical review over the past decade, *Journal of Water Process Engineering* 35 (2020) 101241. Doi: 10.1016/j.jwpe.2020.101241
- [2]. Y.H. Kotp, Removal of organic pollutants using polysulfone ultrafiltration membrane containing polystyrene silicomolybdate nanoparticles: Case study: Borg El Arab area, *Journal of Water Process Engineering* 30 (2019) 100553. Doi: 10.1016/j.jwpe.2018.01.008
- [3]. Y. Ren, Y. Ma, G. Min, W. Zhang, L. Lv, W. Zhang, A mini review of multifunctional ultrafiltration membranes for wastewater decontamination: Additional functions of adsorption and catalytic oxidation, *Science of The Total Environment* 762 (2021) 143083. Doi: 10.1016/j.scitotenv.2020.143083
- [4]. M.D. Garba, M. Usman, M.A.J. Mazumder, A. Al-Ahmed, Inamuddin, Complexing agents for metal removal using ultrafiltration membranes: a review,

- Environmental Chemistry Letters 17 (2019) 1195–1208. Doi: 10.1016/j.desal.2007.01.149
- [5]. Y. Zhang, Q. Fu, Algal fouling of microfiltration and ultrafiltration membranes and control strategies: A review, Separation and Purification Technology 203 (2018) 193-208. Doi: 10.1016/j.seppur.2018.04.040
- [6]. P. Kaner, E. Rubakh, D.H. Kim, A. Asatekin, Zwitterion-containing polymer additives for fouling resistant ultrafiltration membranes, Journal of Membrane Science 533 (2017) 141-159. Doi: 10.1016/j.memsci.2017.03.034
- [7]. X. Shi, G. Tal, N.P. Hankins, V. Gitis, Fouling and cleaning of ultrafiltration membranes: A review, Journal of Water Process Engineering 1 (2014) 121-138. Doi: 10.1016/j.jwpe.2014.04.003
- [8]. M.J. Corbatón-Báguena, S. Álvarez-Blanco, M.C. Vincent-Vela, Cleaning of ultrafiltration membranes fouled with BSA by means of saline solutions, Separation and Purification Technology 125 (2014) 1-10. Doi: 10.1016/j.seppur.2014.01.035
- [9]. K. Li, S. Li, T. Huang, C. Dong, J. Li, B. Zhao, S. Zhang, Chemical cleaning of ultrafiltration membrane fouled by humic substances: Comparison between hydrogen peroxide and sodium hypochlorite, International Journal of Environmental Research and Public Health 16 (2019) 2568. Doi: 10.3390/ijerph16142568
- [10]. A. Behboudi, Y. Jafarzadeh, R. Yegani, Polyvinyl chloride/polycarbonate blend ultrafiltration membranes for water treatment, Journal of Membrane Science 534 (2017) 18-24. Doi: 10.1016/j.memsci.2017.04.011
- [11]. S. Mokhtari, A. Rahimpour, A.A. Shamsabadi, S. Habibzadeh, M. Soroush, Enhancing performance and surface antifouling properties of polysulfone ultrafiltration membranes with salicylate-alumoxane nanoparticles, Applied Surface Science 393 (2017) 93-102. Doi: 10.1016/j.apsusc.2016.10.005
- [12]. E.S. Awad, T.M. Sabirova, N.A. Tretyakova, Q.F. Alsalhy, A. Figoli, I.K. Salih, A mini-review of enhancing ultrafiltration membranes (UF) for wastewater treatment: Performance and stability, ChemEngineering 5 (2021) 34. Doi: 10.3390/chemengineering5030034
- [13]. U.W.R. Siagian, K. Khoiruddin, A.K. Wardani, P.T.P. Aryanti, I.N. Widiasta, G. Qiu, Y.P. Ting, I.G. Wenten, High-performance ultrafiltration membrane: Recent progress and its application for wastewater treatment, Current Pollution Reports 7 (2021) 448–462. Doi: 10.1007/s40726-021-00204-5
- [14]. V. Vatanpour, S. Faghani, R. Keyikoglu, A. Khataee, Enhancing the permeability and antifouling properties of cellulose acetate ultrafiltration membrane by incorporation of ZnO@graphitic carbon nitride nanocomposite, Carbohydrate Polymers 256 (2021) 117413. Doi: 10.1016/j.carbpol.2020.117413
- [15]. M.S.S.A. Saraswathi, D. Rana, S. Alwarappan, S. Gowrishankar, P. Kanimozhi, A. Nagendran, Cellulose acetate ultrafiltration membranes customized with bio-inspired polydopamine coating and in situ immobilization of silver nanoparticles, New Journal of Chemistry 423 (2019) 4216-4225. Doi: 10.1039/C8NJ04511A
- [16]. S. Yang, T. Wang, R. Tang, Q. Yan, W. Tian, L. Zhang, Enhanced permeability, mechanical and antibacterial properties of cellulose acetate ultrafiltration membranes incorporated with lignocellulose nanofibrils, International Journal of Biological Macromolecules, 151 (2020) 159-167. Doi: 10.1016/j.ijbiomac.2020.02.124
- [17]. Z.J. Lu, T. Lin, W. Chen, X.B. Zhang, Influence of KMnO_4 preoxidation on ultrafiltration performance and membrane material characteristics, Journal of Membrane Science 486 (2015) 49-58. Doi: 10.1016/j.memsci.2015.03.042
- [18]. H. Kaur, V.K. Bulasara, R.K. Gupta, Influence of pH and temperature of dip-coating solution on the properties of cellulose acetate-ceramic composite membrane for ultrafiltration, Carbohydrate Polymers 195 (2018) 613-621. Doi: 10.1016/j.carbpol.2018.04.121
- [19]. G.W. Snedecor, W.G. Cochran, Statistical methods, 8th ed., Iowa State University Press, Iowa, USA, 1989.
- [20]. W.K. Härdle, L. Simar, Applied Multivariate Statistical Analysis, 5th ed., Springer Nature, Switzerland, 2019.

Received: 22.02.2022

Received in revised form: 04.04.2022

Accepted: 21.04.2022